U. S. Department of Energy – National Energy Technology Laboratory (NETL)
2023 Virtual Workshop on Multiphase Flow Science – Morgantown-WV-USA – August 1-2, 2023

Scale sensitive sub-grid models for effective drag, filtered and residual stresses in fluidized gas-particle flows

Chris C. Milioli, Fernando E. Milioli
University of São Paulo - Brazil

At the 2021 NETL Multiphase Flow Science workshop we presented:

On the effect of particle Froude number in sub-grid modeling of gas-solid fluidized flows

Among the conclusions of that work we stated that:

Before new sub-grid models could be derived accounting for particle Froude number, further work would be required to account for:

higher domain average gas Reynolds numbers
a variety of domain average solid volume fractions

Those goals have been achieved, and related outcomes are now exposed in two presentations:

1) Results accounting for ranges of domain average gas Reynolds numbers and solid volume fractions, for a range of particle Froude numbers
2) New sub-grid models for effective drag, filtered and residual stresses

Presentation (2) follows next.

Filtered two-fluid modeling

We ultimately aim to provide sub-grid models for filtered two-fluid modeling.

$$\frac{\partial}{\partial t}\left(\rho_g\bar{\phi}_g\right) + \nabla\cdot\left(\rho_g\bar{\phi}_g\tilde{\boldsymbol{v}}_g\right) = 0 \qquad \frac{\partial}{\partial t}\left(\rho_s\bar{\phi}_s\right) + \nabla\cdot\left(\rho_s\bar{\phi}_s\tilde{\boldsymbol{v}}_s\right) = 0$$

$$\frac{\partial}{\partial t}\left(\rho_g\bar{\phi}_g\tilde{\boldsymbol{v}}_g\right) + \nabla\cdot\left(\rho_g\bar{\phi}_g\tilde{\boldsymbol{v}}_g\tilde{\boldsymbol{v}}_g\right) = -\bar{\phi}_g\nabla\cdot\tilde{\boldsymbol{\sigma}}_g - \nabla\cdot\boldsymbol{\tau}'_g - \bar{\boldsymbol{M}}_I + \rho_g\bar{\phi}_g\boldsymbol{g}$$

$$\frac{\partial}{\partial t}\left(\rho_s\bar{\phi}_s\tilde{\boldsymbol{v}}_s\right) + \nabla\cdot\left(\rho_s\bar{\phi}_s\tilde{\boldsymbol{v}}_s\tilde{\boldsymbol{v}}_s\right) = -\nabla\cdot\bar{\boldsymbol{\sigma}}_s - \nabla\cdot\boldsymbol{\tau}'_s - \bar{\phi}_s\nabla\cdot\tilde{\boldsymbol{\sigma}}_g + \boldsymbol{B}'_{gs} + \bar{\boldsymbol{M}}_I + \rho_s\bar{\phi}_s\boldsymbol{g}$$

$$\bar{\boldsymbol{M}}_I = (1-H)\bar{\beta}\left(\tilde{\boldsymbol{v}}_g - \tilde{\boldsymbol{v}}_s\right)$$

$$\tilde{\boldsymbol{\sigma}}_g = \left[\tilde{P}_g - \left(\lambda_g + \tfrac{2}{3}\mu_g\right)\left(\nabla\cdot\tilde{\boldsymbol{v}}_g\right)\right]\boldsymbol{I} - 2\mu_g\tilde{\boldsymbol{S}}_g$$

$$\bar{\boldsymbol{\sigma}}_s = \left[\bar{P}_s - \overline{\left(\lambda_s + \tfrac{2}{3}\mu_s\right)\left(\nabla\cdot\boldsymbol{v}_s\right)}\right]\boldsymbol{I} - 2\bar{\mu}_s\tilde{\boldsymbol{S}}_s = P_{fil,s}\boldsymbol{I} - 2\mu_{fil,s}\tilde{\boldsymbol{S}}_s$$

$$\boldsymbol{\tau}'_\ell = \rho_\ell\bar{\phi}_\ell\widetilde{\boldsymbol{v}_\ell\boldsymbol{v}_\ell} - \rho_\ell\bar{\phi}_\ell\tilde{\boldsymbol{v}}_\ell\tilde{\boldsymbol{v}}_\ell = P_{res,\ell}\boldsymbol{I} - 2\mu_{res,\ell}\tilde{\boldsymbol{S}}_\ell$$

$$\tilde{\boldsymbol{S}}_\ell = \tfrac{1}{2}\left[\nabla\tilde{\boldsymbol{v}}_\ell + \left(\nabla\tilde{\boldsymbol{v}}_\ell\right)^T\right] - \tfrac{1}{3}\left(\nabla\cdot\tilde{\boldsymbol{v}}_\ell\right)\boldsymbol{I}$$

Effective, filtered and residual closures

$$H = 1 - \frac{\beta_{eff}}{\bar{\beta}} \qquad \beta_{eff} = \frac{\overline{\beta\left(\boldsymbol{v}_g - \boldsymbol{v}_s\right)}}{\left(\tilde{\boldsymbol{v}}_g - \tilde{\boldsymbol{v}}_s\right)}$$

$$P_{fil,s} = \tfrac{1}{3}\mathrm{tr}\left[\bar{P}_s - \overline{\left(\lambda_s + \tfrac{2}{3}\mu_s\right)\left(\nabla\cdot\boldsymbol{v}_s\right)}\right]$$

$$\mu_{fil,s} = \bar{\mu}_s$$

$$P_{res,\ell} = \tfrac{1}{3}\mathrm{tr}\left(\boldsymbol{\tau}'_\ell\right)$$

$$\mu_{res,\ell} = \frac{\left|\boldsymbol{\tau}'_{shear,\ell}\right|}{2\left|\tilde{\boldsymbol{S}}_{shear,\ell}\right|}$$

We go for effective, filtered and residual parameters by filtering over predictions from highly resolved simulations (HRS) with microscopic two-fluid modeling.

Microscopic two-fluid modeling

On the basis of Anderson and Jackson' formulation, with microscopic closures as implemented into the MFIX code by Agrawal et al. (2001).

$$\frac{\partial}{\partial t}\left(\rho_g \phi_g\right) + \nabla\cdot\left(\rho_g \phi_g \boldsymbol{v}_g\right) = 0$$

$$\frac{\partial}{\partial t}\left(\rho_s \phi_s\right) + \nabla\cdot\left(\rho_s \phi_s \boldsymbol{v}_s\right) = 0$$

$$\frac{\partial}{\partial t}\left(\rho_g \phi_g \boldsymbol{v}_g\right) + \nabla\cdot\left(\rho_g \phi_g \boldsymbol{v}_g \boldsymbol{v}_g\right) = -\phi_g \nabla\cdot\boldsymbol{\sigma}_g - \boldsymbol{M}_I + \rho_g \phi_g \boldsymbol{g}$$

$$\frac{\partial}{\partial t}\left(\rho_s \phi_s \boldsymbol{v}_s\right) + \nabla\cdot\left(\rho_s \phi_s \boldsymbol{v}_s \boldsymbol{v}_s\right) = -\nabla\cdot\boldsymbol{\sigma}_s - \phi_s \nabla\cdot\boldsymbol{\sigma}_g + \boldsymbol{M}_I + \rho_s \phi_s \boldsymbol{g}$$

$$\boldsymbol{M}_I = \beta\left(\boldsymbol{v}_g - \boldsymbol{v}_s\right)$$

$$\boldsymbol{\sigma}_\ell = \left[P_\ell - \left(\lambda_\ell + \tfrac{2}{3}\mu_\ell\right)\left(\nabla\cdot\boldsymbol{v}_\ell\right)\right]\boldsymbol{I} - 2\mu_\ell \boldsymbol{s}_\ell$$

$$\boldsymbol{s}_\ell = \tfrac{1}{2}\left[\nabla\boldsymbol{v}_\ell + \left(\nabla\boldsymbol{v}_\ell\right)^T\right] - \tfrac{1}{3}\left(\nabla\cdot\boldsymbol{v}_\ell\right)\boldsymbol{I}$$

Microscopic closures

Drag

Wen and Yu (1966)

Solid phase pressure and viscous stresses

Lun et al. (1984),
as adapted by Agrawal et al. (2001)

Highly resolved simulations (MFIX) / filtering

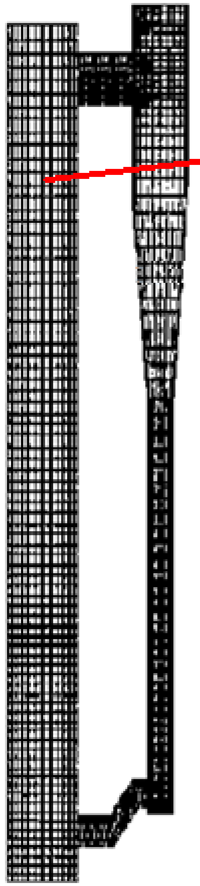

LSS

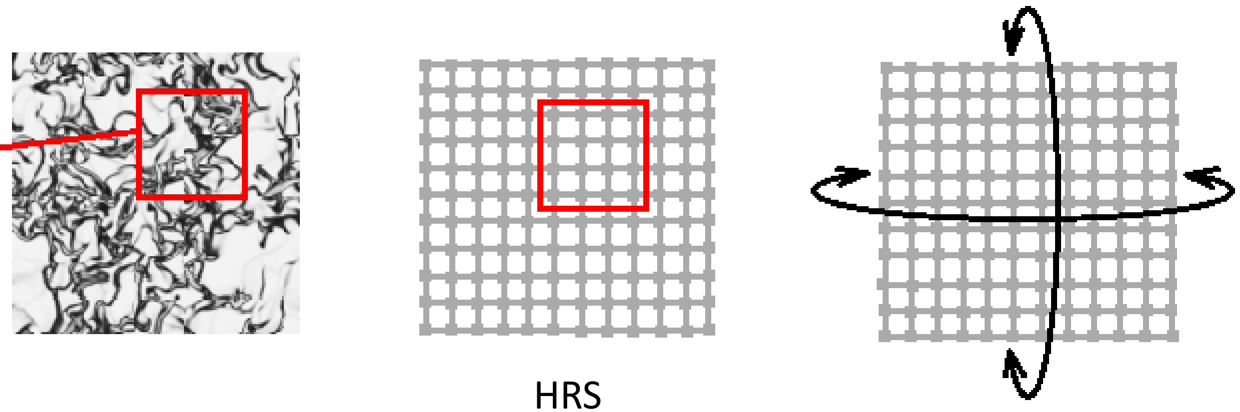

- All periodic boundaries
- 16 x 16 cm domain
- 128 x 128 grids
- 1.25 x 1.25 mm grid cells
- up to 4 x 4 cm filter sizes

d_p	40 / 75 / 150 / 300 μm
$Fr_p = v_t^2 / (g d_p)$	12.21 / 64.85 / 286.69 / 799.22
ρ_s	1500 kg/m^3
e	0.9
ρ_g	1.3 kg/m^3
μ_g	1.8×10^{-5} kg/(m s)
$\langle \phi_s \rangle$	0.05 / 0.15 / 0.25 / 0.35 / 0.45 / 0.55
$\langle Re_g \rangle / \langle Re_g \rangle_{susp}$	1 / 8.15 / 16.30 / 24.45

Filtered data classified by narrow ranges of

$\bar{\phi}_s$, $\tilde{v}_{slip,y}$

Results

$$\tilde{v}^*_{slip,y} = \left|\tilde{v}_{slip,y}/v_{t75}\right|$$

$$\Delta^*_f = \Delta_f/\left(v^2_{t75}/g\right)$$

$$Fr_p = v^2_t/\left(g d_p\right)$$

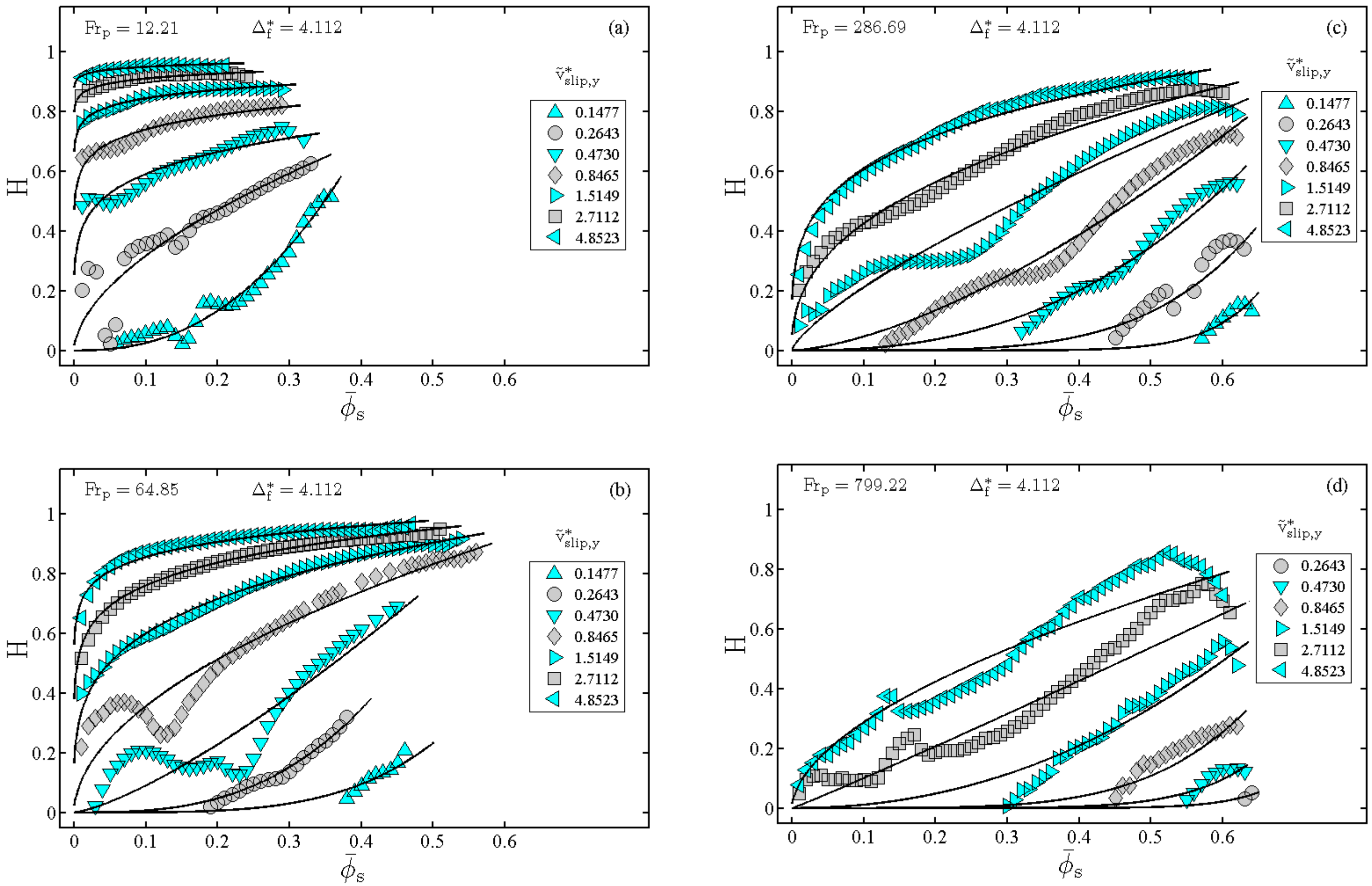

$$H = \min[H_1 , H_2]$$

$$H_1 = \left(a_1 + \frac{a_2}{\left(\tilde{v}^*_{slip,y}\right)} + \frac{a_3}{\left(\tilde{v}^*_{slip,y}\right)^2} \right) \bar{\phi}_s^{\left(b_1 + \frac{b_2}{\left(\tilde{v}^*_{slip,y}\right)} + \frac{b_3}{\left(\tilde{v}^*_{slip,y}\right)^2} \right)}$$

$$H_2 = c_1 + c_2 \bar{\phi}_s$$

The various coefficients were presented in numerical form since no precise enough mathematical rules of correlation could be found.

$\tilde{v}^*_{slip,y} < 0.8$

Fr_p	Δ^*_f	a_1	a_2	a_3	b_1	b_2	b_3	c_1	c_2
	1.028	0.9854	- 0.2496	0.02155	0.2483	- 0.04851	0.01608	1.6250	- 3.1250
	2.056	1.3470	- 0.3945	0.07045	0.2037	- 0.08908	0.04547	3.0769	- 7.6923
12.21	4.112	3.0220	- 1.6890	0.3178	0.2862	- 0.2219	0.07850	1.9583	- 4.1667
	6.168	3.2150	- 1.7820	0.3271	0.3906	- 0.2859	0.08462	1.7143	- 3.5714
	8.224	3.3330	- 1.8660	0.3409	0.4024	- 0.2989	0.08604	1.5313	- 3.1250
	1.028	1.7040	- 0.5144	0.05743	1.5330	- 0.3026	0.0701	5.0833	- 8.3333
	2.056	5.9680	- 3.2330	0.5615	1.4590	- 0.3163	0.1287	14.2500	- 25.0000
64.85	4.112	- 5.2010	4.3050	- 0.4414	- 1.5430	1.6020	- 0.1158	17.6667	- 33.3333
	6.168	- 8.9100	5.5750	- 0.2332	- 2.2630	1.8720	- 0.1006	10.0000	- 20.0000
	8.224	45.1000	- 34.5600	6.6860	- 1.2540	1.1070	0.03978	16.3333	- 33.3333
	1.028	0.8370	- 0.2250	0.01917	1.6980	- 0.1343	0.01282	4.6154	- 7.6923
	2.056	2.5740	- 0.5549	0.1240	1.0660	0.7769	0.01280	8.8571	- 14.2857
286.69	4.112	3.6660	- 1.6480	0.3834	0.4496	0.7892	0.07359	12.8000	- 20.0000
	6.168	10.3600	- 6.9670	1.4820	- 0.3457	1.2150	0.08068	21.3333	- 33.3333
	8.224	21.9600	-16.1200	3.2460	- 1.0910	1.6000	0.07133	16.0000	- 25.0000
	1.028	40.4200	- 22.9900	3.5350	11.5700	- 3.2870	0.5080	1.1636	- 1.8182
	2.056	0.1136	0.4505	- 0.01229	0.08879	1.8980	- 0.1001	4.5714	- 7.1429
799.22	4.112	1.6550	0.9124	0.04843	1.0920	3.2500	- 0.1753	12.4000	- 20.0000
	6.168	24.1600	- 51.7000	28.4400	3.3310	- 3.3320	3.6430	8.8571	- 14.2857
	8.224	0.2778	3.1140	0.2333	- 0.4787	4.8970	- 0.04863	10.3333	- 16.6667

$\tilde{v}^*_{slip,y} \geq 0.8$

Fr_p	Δ^*_f	a_1	a_2	a_3	b_1	b_2	b_3	c_1	c_2
	1.028	0.9936	0.01384	- 0.1084	0.00261	0.2264	- 0.03508	1.6250	- 3.1250
	2.056	1.0030	- 0.06721	0.001259	0.0006804	0.1089	0.005454	3.0769	- 7.6923
12.21	4.112	1.0050	- 0.1141	0.02910	0.0007523	0.06413	0.009367	1.9583	- 4.1667
	6.168	0.9815	- 0.04778	- 0.005081	- 0.008357	0.07968	- 0.004212	1.7143	- 3.5714
	8.224	1.0260	- 0.2034	0.1048	0.005166	0.02557	0.0320	1.5313	- 3.1250
	1.028	1.0890	- 0.05508	0.02728	0.05604	0.7911	- 0.07715	5.0833	- 8.3333
	2.056	1.0690	- 0.06079	0.1826	0.03451	0.4012	0.1231	14.2500	- 25.0000
64.85	4.112	1.0380	- 0.03234	0.1445	0.02561	0.2478	0.1500	17.6667	- 33.3333
	6.168	1.0360	- 0.08281	0.1976	0.02734	0.1685	0.1924	10.0000	- 20.0000
	8.224	1.0320	- 0.1124	0.2470	0.02838	0.1181	0.2365	16.3333	- 33.3333
	1.028	1.3570	- 1.6210	0.6979	0.6291	0.1795	- 0.02427	4.6154	- 7.6923
	2.056	1.1690	- 0.1748	0.4089	0.1745	1.0320	0.2343	8.8571	- 14.2857
286.69	4.112	1.0970	- 0.1998	0.5041	0.07632	0.7575	0.3945	12.8000	- 20.0000
	6.168	1.0510	- 0.02845	0.4537	0.02634	0.8111	0.3702	21.3333	- 33.3333
	8.224	1.0170	0.1761	0.2892	- 0.009139	0.9301	0.2604	16.0000	- 25.0000
	1.028	1.1400	- 2.9500	2.3110	2.0100	- 5.8210	5.7340	1.1636	- 1.8182
	2.056	0.8188	1.9540	- 0.8404	- 0.02071	4.4780	- 0.9635	4.5714	- 7.1429
799.22	4.112	1.1010	- 0.6132	1.7310	0.07201	2.0530	1.5660	12.4000	- 20.0000
	6.168	0.5055	3.9500	- 1.7140	- 0.4612	5.4510	- 1.0690	8.8571	- 14.2857
	8.224	0.8726	1.6800	1.0220	- 0.3450	4.5040	0.1909	10.3333	- 16.6667

UNIVERSIDADE DE SÃO PAULO
SCIENTIA VINCES

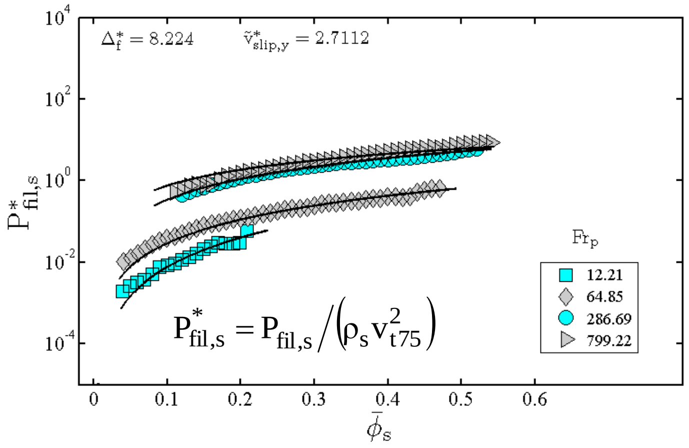

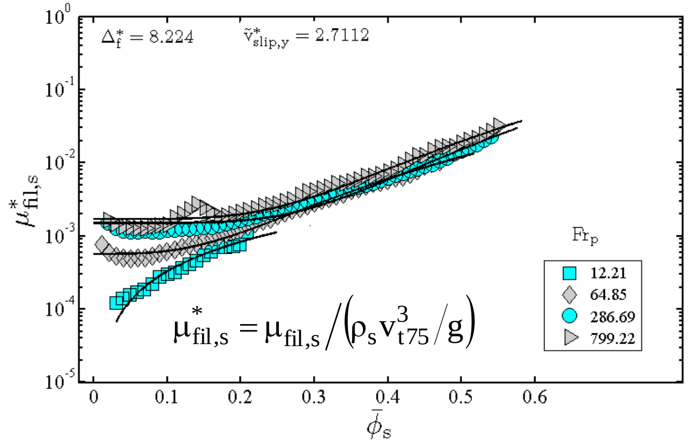

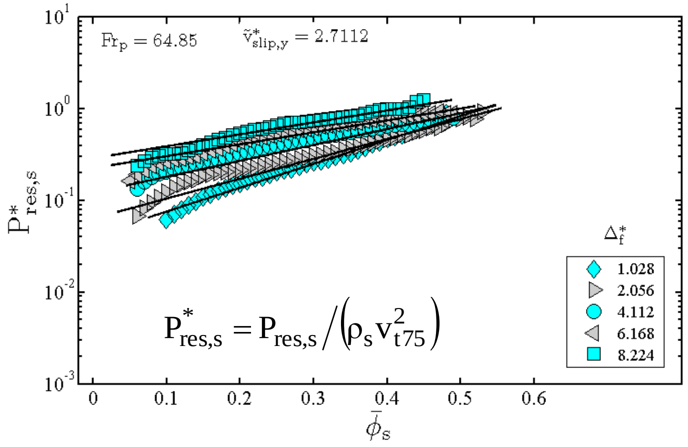

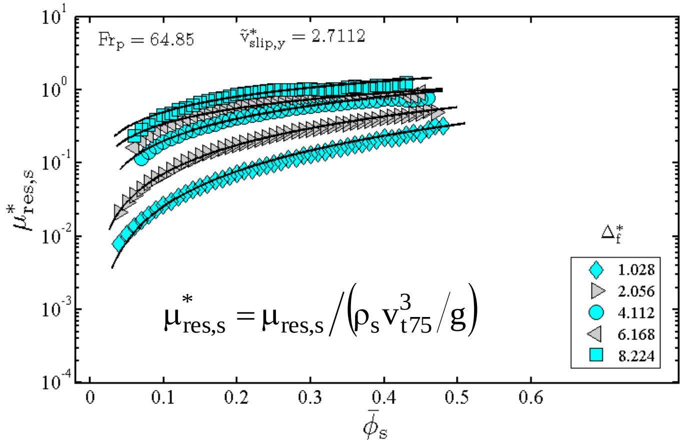

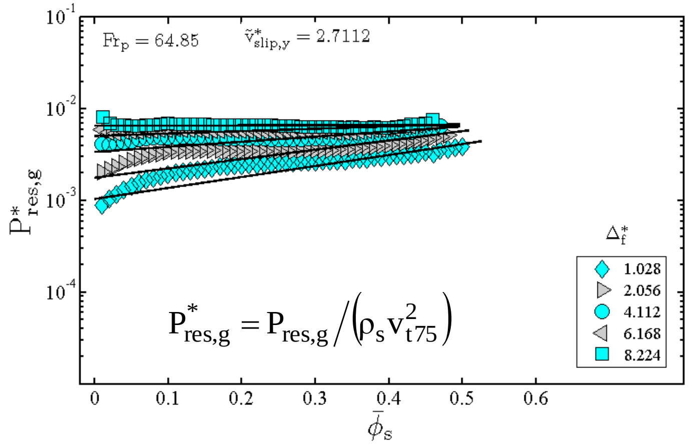

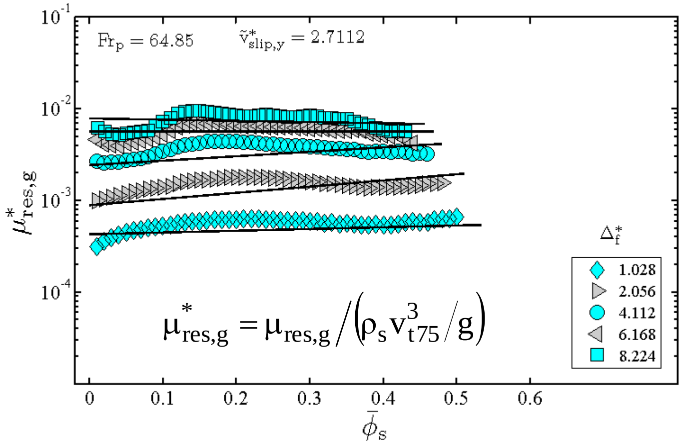

$$P^*_{fil,s}\ ;\ \mu^*_{fil,s}\ ;\ \mu^*_{res,s} = \left[a_1\left(\tilde{v}^*_{slip,y}\right)^{a_2} + a_3\right]\bar{\phi}_s^{\left[b_1\left(\tilde{v}^*_{slip,y}\right)^{b_2} + b_3\right]} + c_1$$

$$P^*_{res,s} = \left[a_1\left(\tilde{v}^*_{slip,y}\right)^{a_2} + a_3\right]\exp\left\{\left[b_1\left(\tilde{v}^*_{slip,y}\right)^{b_2} + b_3\right]\bar{\phi}_s\right\}$$

$$P^*_{res,g}\ ;\ \mu^*_{res,g} = \left[a_1\left(\tilde{v}^*_{slip,y}\right)^2 + a_2\left(\tilde{v}^*_{slip,y}\right) + a_3\right]\exp\left\{\left[b_1\left(\tilde{v}^*_{slip,y}\right)^{b_2} + b_3\right]\bar{\phi}_s\right\}$$

Aiming for a smaller set of equations, we correlate only to a most influential third parameter (in addition to the meso-scale markers):

Fr_p for $P^*_{fil,s}$ $\mu^*_{fil,s}$

Δ^*_f for $P^*_{res,s}$ $\mu^*_{res,s}$ $P^*_{res,g}$ $\mu^*_{res,g}$

The various coefficients were presented in numerical form since no precise enough mathematical rules of correlation could be found.

	Fr_p	a_1	a_2	a_3	b_1	b_2	b_3	c_1
$P^*_{fil,s}$	12.21	5.805e-2	3.505e0	5.811e-4	- 2.963e1	- 3.012e-2	3.115e1	0.0
	64.85	2.648e-1	2.251e0	0.0	- 2.887e0	- 2.709e-1	4.135e0	0.0
	286.69	2.302e-6	1.567e1	2.846e0	2.626e-1	1.477e0	5.498e-1	0.0
	799.22	0,0	0,0	1.490e1	0.0	0.0	1.2957e0	0.0
$\mu^*_{fil,s}$	12.21	2.831e-3	1.000e0	- 3.427e-4	- 7.160e-2	- 1.440e0	1.366e0	0.0
	64.85	3.987e-2	1.000e0	8.183e-3	- 1.004e-1	1.211e0	3.669e0	5.700e-4
	286.69	2.295e-1	8.817e-1	- 6.087e-2	- 1.049e-1	- 2.600e0	5.162e0	1.500e-3
	799.22	2.408e-3	4.990e0	6.539e-2	4.940e-1	1.517e0	2.280e0	1.700e-3

	Δ^*_f	a_1	a_2	a_3	b_1	b_2	b_3	c_1
$P^*_{res,s}$	1.028	1.070e-2	1.321e0	1.742e-3	0.0	0.0	6.000e0	–
	2.056	3.422e-1	6.362e-2	- 3.008e-1	0.0	0.0	5.000e0	–
	4.112	3.682e-1	8.971e-2	- 2.806e-1	0.0	0.0	4.000e0	–
	6.168	2.261e-1	2.381e-1	- 6.050e-2	0.0	0.0	3.000e0	–
	8.224	9.972e-2	6.553e-1	9.870e-2	0.0	0.0	3.000e0	–
$\mu^*_{res,s}$	1.028	3.712e-1	1.000e0	1.508e-2	5.193e0	5.000e-2	- 3.856e0	0.0
	2.056	1.225e0	3.900e-1	- 3.836e-1	- 1.282e-1	- 9.438e-1	1.350e0	0.0
	4.112	1.131e0	3.725e-1	3.709e-1	0.0	0.0	1.000e0	0.0
	6.168	4.255e-1	4.626e-1	1.041e0	0.0	0.0	7.000e-1	0.0
	8.224	1.903e-1	1.326e0	1.769e0	0.0	0.0	7.000e-1	0.0
$P^*_{res,g}$	1.028	1.847e-4	- 1.943e-4	2.113e-4	- 4.935e-1	- 1.565e0	2.865e0	–
	2.056	2.423e-4	- 2.688e-4	7.239e-4	- 5.492e0	- 3.458e-1	6.235e0	–
	4.112	1.263e-3	- 3.373e-3	3.259e-3	- 2.817e0	-7.000e-1	2.681e0	–
	6.168	1.778e-3	- 4.722e-3	4.818e-3	- 2.825e0	- 7.000e-1	2.003e0	–
	8.224	2.106e-3	- 5.653e-3	6.413e-3	- 4.537e0	- 4.500e-1	2.935e0	–
$\mu^*_{res,g}$	1.028	- 6.672e-6	1.416e-4	9.345e-5	- 6.489e1	- 1.000e-2	6.469e1	–
	2.056	7.645e-5	- 6.980e-5	5.178e-4	- 2.988e0	- 4.388e-1	3.485e0	–
	4.112	6.027e-4	- 1.523e-3	2.137e-3	- 1.132e0	- 1.037e0	1.519e0	–
	6.168	1.405e-3	- 3.069e-3	3.685e-3	- 1.379e-2	- 4.000e0	- 1.336e-3	–
	8.224	1.823e-3	- 3.886e-3	5.017e-3	- 1.536e-1	- 2.078e0	- 2.829e-1	–

Conclusions

- Accounting of the proposed sub-grid models:
  - ✓ At the meso-scale: $\overline{\phi}_s$, $\tilde{v}^*_{slip,y}$ and Δ^*_f
  - ✓ At the micro-scale: Fr_p
  - ✓ At the macro-scale: $\langle \phi_s \rangle$ and $\langle Re_g \rangle$ (in average)

- Possible improvements:
  - ✓ Account for alternative or additional micro-scale markers
  - ✓ Further assess number and type of meso-scale markers
  - ✓ Correlate to macro-scale markers

(refer to companion presentation for behavior analysis)

Acknowledgements

This work was supported by

CNPq FAPESP

Please direct any questions to milioli@sc.usp.br

Thank you very much!